# Calibration Method of Gain-Phase Errors in Super-resolution Direction Finding for Wideband Signals

Jiaqi Zhen(✉), Danyang Qin, Jie Yang, and Yanchao Li

College of Electronic Engineering, Heilongjiang University, Harbin 150080, China
zhenjiaqi2011@163.com

**Abstract.** Most super-resolution direction finding methods need to know the array manifold exactly, but there is usually gain and phase errors in the array, which directly lead to the discordance of the channels. The paper proposed a novel calibration method in super-resolution direction finding for wideband signals based on spatial domain sparse optimization when gain and phase errors exist. First, the optimization functions are founded by the signals of every frequency, then the functions are optimized iteratively, consequently the information of all frequencies is integrated for the calibration, thus, the actual directions of arrival (DOA) can be estimated. Simulations have proved the method is appropriate for low signal to noise ratio (SNR) and small samples.

**Keywords:** Super-resolution direction finding · Array calibration · Gain-phase errors · Wideband signals

## 1 Introduction

Super-resolution direction finding is one of the major research contents in array signal processing, it is widely used in radio monitoring [1–7] and internet of things [8, 9]. Most of the direction finding methods need to know the accurate array manifold, but there are often amplifiers in the channels, the gains of them are not consistent, and sometimes accompanied with discordant lengths of the channels in practical systems, which directly lead to the performance deteriorated of direction finding methods, and even failure, so they are necessary to be calibrated.

Gain-phase errors have no relation with DOA of the signal, they are caused by the different responses of the channels. Srinath [10] analyzed the effect of the gain and phase errors on traditional multiple signal classification (MUSIC) [11] algorithm, he proved that they have a great influence on the estimation, even lead to the failure. Most of the calibration methods are based on eigenstructure and lack adaptation to the

J. Zhen—This work was supported by the National Natural Science Foundation of China under Grant No. 61501176 and 61302074, Specialized Research Fund for the Doctoral Program of Higher Education under Grant No. 20122301120004, Natural Science Foundation of Heilongjiang Province under Grant No. QC2013C061.


X.-L. Huang (Ed.): MLICOM 2016, LNICST 183, pp. 303–313, 2017.
DOI: 10.1007/978-3-319-52730-7_31

background of low signal to noise ratio (SNR) and small samples. Wang [12] proposed a simple and fast calibration algorithm that does not require any prior knowledge of the DOA along with sensor gain and phase uncertainties based on Toeplize characteristic; Jiang [13] provided the conventional and improved data models, then correct the array, the estimation accuracy is not affected regardless of how large the phase errors are; Xu [14] estimated DOA of strong and weak signals in the presence of array gain and phase mismatch; Cao and Ye [15] proposed a calibration method for channel gain and phase uncertainties based on fourth-order cumulant technique, it adapts to the background of non-Gaussian signals and Gaussian noise. All the methods above only adapt to narrowband signals, and need many samples, but there are rare published literatures of gain and phase errors calibration for wideband signals.

The paper proposed a novel array error calibration method in super-resolution direction finding for wideband signals based on spatial domain sparse optimization when gain-phase errors exist in the array, the corresponding optimization functions are founded by the signal of every frequency, then the functions are optimized iteratively, at last, the information of all frequencies is integrated to calibrated the errors, consequently the actual DOA can be acquired.

## 2 Signal Model

### 2.1 Ideal Signal Model

It is seen from Fig. 1, suppose there are $K$ far-field wideband signals $s_k(t)$ $(k = 1, 2, \cdots, K)$ impinging on the uniform linear array composed of $M$ omnidirectional sensors, the space of them is $d$, it is equal to half of the wavelength of the center frequency, DOAs of them are $\boldsymbol{\alpha} = [\alpha_1, \cdots, \alpha_k, \cdots, \alpha_K]$, the first sensor is defined as the reference, then output of the $m$th sensor can be written as

$$x_m(t) = \sum_{k=1}^{K} s_k(t - \tau_m(\alpha_k)) + n_m(t), m = 1,\ 2, \cdots, M \tag{1}$$

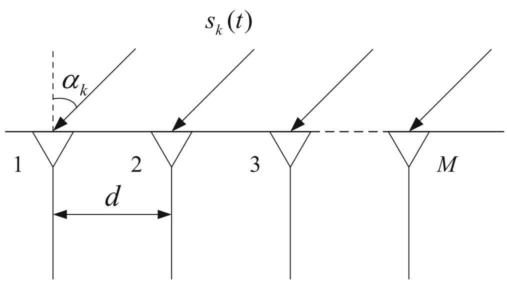


**Fig. 1.** Array signal Model

Where $\tau_m(\alpha_k) = (m-1)\frac{d}{c}\sin\alpha_k$ is the propagation delay for the $k$th signal arriving at the $m$th sensor with respect to the reference of the array, $c$ is the propagating speed of the signal, $n_m(t)$ is the Gaussian white noise on the $m$th sensor.

Assume that the range of the frequency band of all signals is $[f_{\mathrm{Low}}, f_{\mathrm{High}}]$, before the processing, we divide the output vector into $J$ nonoverlapping components, Discrete Fourier Transform(DFT) is performed on (1) and the array outputs of $J$ frequencies can be represented as

$$\boldsymbol{X}(f_i) = \boldsymbol{A}(f_i, \alpha)\boldsymbol{S}(f_i) + \boldsymbol{N}(f_i) \quad i = 1, 2, \cdots, J \tag{2}$$

Where $f_{\mathrm{Low}} \le f_i \le f_{\mathrm{High}}$ $(i = 1, 2, \cdots, J)$, $KP$ snapshots are collected at every frequency, then we have

$$\boldsymbol{X}(f_i) = [\boldsymbol{X}_1(f_i), \cdots, \boldsymbol{X}_m(f_i), \cdots, \boldsymbol{X}_M(f_i)]^{\mathrm{T}} \tag{3}$$

Where

$$\boldsymbol{X}_m(f_i) = [X_m(f_i, 1), \cdots, X_m(f_i, kp), \cdots, X_m(f_i, KP)] \tag{4}$$

$\boldsymbol{A}(f_i, \boldsymbol{\alpha})$ is a $M \times K$ dimensional steering vector

$$\boldsymbol{A}(f_i, \boldsymbol{\alpha}) = [\boldsymbol{a}(f_i, \alpha_1), \cdots, \boldsymbol{a}(f_i, \alpha_k), \cdots, \boldsymbol{a}(f_i, \alpha_K)] \tag{5}$$

$$\boldsymbol{a}(f_i, \alpha_k) = \left[1, \exp(-\mathrm{j}2\pi f_i \frac{d}{c}\sin\alpha_k), \cdots, \exp\left(-\mathrm{j}(M-1)2\pi f_i \frac{d}{c}\sin\alpha_k\right)\right]^{\mathrm{T}} \tag{6}$$

And

$$\boldsymbol{S}(f_i) = [\boldsymbol{S}_1(f_i), \cdots, \boldsymbol{S}_k(f_i), \cdots, \boldsymbol{S}_K(f_i)]^{\mathrm{T}} \tag{7}$$

is the signal vector matrix after DFT to $s_k(t)$ $(k = 1, 2, \cdots, K)$, where

$$\boldsymbol{S}_k(f_i) = [S_k(f_i, 1), \cdots S_k(f_i, kp), \cdots, S_k(f_i, KP)] \tag{8}$$

Here, $S_k(f_i, kp)$ is the $kp$th snapshots of the $k$th signal at $f_i$, then

$$\boldsymbol{N}(f_i) = [\boldsymbol{N}_1(f_i), \cdots, \boldsymbol{N}_m(f_i), \cdots, \boldsymbol{N}_M(f_i)]^{\mathrm{T}} \tag{9}$$

$$\boldsymbol{N}_m(f_i) = [N_m(f_i, 1), \cdots, N_m(f_i, kp), \cdots, N_m(f_i, KP)] \tag{10}$$

is the noise vector after performing DFT on $n_m(t)$ $(m = 1, 2, \cdots, M)$ with mean 0 and variance $\mu^2(f_i)$.

### 2.2 Gain-Phase Errors Model

For convenience, we only discuss the information at frequency $f_i$ for the moment. When there is only gain and phase errors in the array, $\boldsymbol{W}(f_i)$ is defined as perturbation matrix, it is

$$\boldsymbol{W}(f_i) = \mathrm{diag}\Big([1,\ W_2(f_i), \cdots, W_m(f_i), \cdots, W_M(f_i)]^{\mathrm{T}}\Big) \tag{11}$$

Here

$$W_m(f_i) = \rho_m(f_i)\mathrm{e}^{\mathrm{j}\varphi_m(f_i)}, m = 1, 2, \cdots, M \tag{12}$$

is the gain and phase perturbation of $m$th sensor, $\rho_m(f_i)$, $\varphi_m(f_i)$ are respectively the gain and phase of the $m$th sensor with respect to the reference sensor, so the perturbed steering vector is

$$\begin{aligned}\boldsymbol{a}'(f_i, \alpha_k) &= [1,\ W_2(f_i)e^{j2\pi f_i \tau_2(\alpha_k)}, \cdots, W_m(f_i)e^{j2\pi f_i \tau_m(\alpha_k)}, \cdots, W_M(f_i)e^{j2\pi f_i \tau_M(\alpha_k)}]^{\mathrm{T}} \\ &= \mathrm{diag}\big([1,\ W_2(f_i), \cdots, W_m(f_i), \cdots, W_M(f_i)]^{T}\big)\, \boldsymbol{a}(f_i, \alpha_k) \\ &= \boldsymbol{W}(f_i)\boldsymbol{a}(f_i, \alpha_k) \quad (k = 1, 2, \cdots, K)\end{aligned} \tag{13}$$

So the corresponding array manifold matrix is

$$\boldsymbol{A}'(f_i, \boldsymbol{\alpha}) = [\boldsymbol{a}'(f_i, \alpha_1), \cdots, \boldsymbol{a}'(f_i, \alpha_k), \cdots, \boldsymbol{a}'(f_i, \alpha_K)] = \boldsymbol{W}(f_i)\boldsymbol{A}(f_i, \boldsymbol{\alpha}) \tag{14}$$

For the sake of simplicity, we also define the gain/phase uncertainty vector among sensors as $\boldsymbol{w}(f_i) = [\rho_2(f_i)e^{j\varphi_2(f_i)}, \cdots, \rho_m(f_i)e^{j\varphi_m(f_i)}, \cdots, \rho_M(f_i)\mathrm{e}^{\mathrm{j}\varphi_M(f_i)}]^{\mathrm{T}}$, so the output of the array at frequency $f_i$ can be expressed as

$$\begin{aligned}\boldsymbol{X}'(f_i) = \boldsymbol{A}'(f_i, \boldsymbol{\alpha})\boldsymbol{S}(f_i) + \boldsymbol{N}(f_i) &= \boldsymbol{W}(f_i)\boldsymbol{A}(f_i, \boldsymbol{\alpha})\boldsymbol{S}(f_i) + \boldsymbol{N}(f_i) \\ &= \boldsymbol{A}(f_i, \boldsymbol{\alpha})\boldsymbol{S}(f_i) + \boldsymbol{\Lambda}(f_i)\boldsymbol{w}(f_i) + \boldsymbol{N}(f_i)\end{aligned} \tag{15}$$

Where $\boldsymbol{\Lambda}(f_i)$ is the vector related to the signal along with gain and phase errors.

## 3 Estimation Theory

We divide the searching area into some grids $\boldsymbol{\Omega} = [\bar{\alpha}_1, \cdots, \bar{\alpha}_l, \cdots, \bar{\alpha}_L]$, here $K<<L$, take $\boldsymbol{\Omega}$ into (2)

$$\bar{\boldsymbol{X}}'(f_i) = \boldsymbol{A}'(f_i, \boldsymbol{\Omega})\bar{\boldsymbol{S}}(f_i) + \boldsymbol{N}(f_i)\ (i = 1, 2, \cdots, J) \tag{16}$$

The covariance matrix is

$$\bar{\boldsymbol{R}}'(f_i) = E\Big\{\bar{\boldsymbol{X}}'(f_i)(\bar{\boldsymbol{X}}'(f_i))^{\mathrm{H}}\Big\}\ (i = 1, 2, \cdots, J) \tag{17}$$

In (16), $\bar{\boldsymbol{S}}(f_i) = [\bar{\boldsymbol{S}}(f_i, 1), \cdots, \bar{\boldsymbol{S}}(f_i, kp), \cdots, \bar{\boldsymbol{S}}(f_i, KP)]$,where $\bar{\boldsymbol{S}}(f_i, kp) = [\bar{S}_1(f_i, kp), \cdots, \bar{S}_l(f_i, kp), \cdots, \bar{S}_L(f_i, kp)]^{\mathrm{T}}$ is a sparse matrix, it only contains $K$ non-zero elements, they are non-zero if and only if $\bar{\alpha}_l = \alpha_k$ and $\bar{S}_l(f_i, kp) = S_k(f_i, kp)\,(l = 1, 2, \cdots, L;\ k = 1, 2, \cdots, K)$, so $\bar{\boldsymbol{S}}(f_i)$ can be regarded as $\boldsymbol{S}(f_i)$ jointed many zero elements.

Define $\boldsymbol{\delta}(f_i) = [\delta_1(f_i), \cdots, \delta_l(f_i), \cdots, \delta_L(f_i)]^T$ as the vector formed by variances of the elements in $\bar{\boldsymbol{S}}(f_i)$, it reflects the energy of the signal, that is

$$\bar{\boldsymbol{S}}(f_i) \sim N(0, \boldsymbol{\Sigma}(f_i)) \tag{18}$$

Where $\boldsymbol{\Sigma}(f_i) = \mathrm{diag}(\boldsymbol{\delta}(f_i))$, as $\bar{\boldsymbol{S}}(f_i)$ is $\boldsymbol{S}(f_i)$ jointed many zero elements, $\boldsymbol{\delta}(f_i)$ contains $K$ non-zero elements too.

It can be seen from (16) and (18), probability density of the output signal at $f_i$ along with the error is

$$\begin{aligned} P\left(\bar{\boldsymbol{X}}'(f_i)\middle|\bar{\boldsymbol{S}}(f_i); \boldsymbol{w}(f_i), \mu^2(f_i)\right) &= \left|\pi\mu^2(f_i)\boldsymbol{I}_M\right|^{-KP}\exp\left\{-\mu^2(f_i)\left\|\bar{\boldsymbol{X}}'(f_i) - \boldsymbol{A}'(f_i, \boldsymbol{\Omega})\bar{\boldsymbol{S}}(f_i)\right\|_2^2\right\} \\ &= \left|\pi\mu^2(f_i)\boldsymbol{I}_M\right|^{-KP}\exp\left\{-\mu^2(f_i)\times\left\|\bar{\boldsymbol{X}}'(f_i) - \boldsymbol{W}(f_i)\boldsymbol{A}(f_i, \boldsymbol{\Omega})\bar{\boldsymbol{S}}(f_i)\right\|_2^2\right\} \end{aligned} \tag{19}$$

Combining (16), (18) and (19), probability density of $\bar{\mathbf{X}}'(f_i)$ is

$$\begin{aligned} & P\left(\bar{\boldsymbol{X}}'(f_i); \boldsymbol{\delta}(f_i), \boldsymbol{w}(f_i), \mu^2(f_i)\right) \\ &= \int P\left(\bar{\boldsymbol{X}}'(f_i)\middle|\bar{\boldsymbol{S}}(f_i); \boldsymbol{w}(f_i), \mu^2(f_i)\right)P(\bar{\boldsymbol{S}}(f_i); \boldsymbol{\delta}(f_i))\mathrm{d}\bar{\boldsymbol{S}}(f_i) \\ &= \left|\pi\left(\mu^2(f_i)\boldsymbol{I}_M + \boldsymbol{A}'(f_i, \boldsymbol{\Omega})\boldsymbol{\Sigma}(f_i)(\boldsymbol{A}'(f_i, \boldsymbol{\Omega}))^H\right)\right|^{-KP} \\ & \exp\left\{-KP \times \mathrm{tr}\left(\left(\mu^2(f_i)\boldsymbol{I}_M + \boldsymbol{A}'(f_i, \boldsymbol{\Omega})\boldsymbol{\Sigma}(f_i)(\boldsymbol{A}'(f_i, \boldsymbol{\Omega}))^H\right)^{-1}\bar{\boldsymbol{R}}'(f_i)\right)\right\} \end{aligned} \tag{20}$$

Then Expectation Maximization (EM) method [16] can be employed to estimate each parameter, compute distribution function of $P\left(\bar{\boldsymbol{X}}'(f_i), \bar{\boldsymbol{S}}(f_i); \boldsymbol{\delta}(f_i), \boldsymbol{w}(f_i), \mu^2(f_i)\right)$, in the E-step:

$$\begin{aligned} & F\left(\bar{\boldsymbol{X}}'(f_i), \bar{\boldsymbol{S}}(f_i); \boldsymbol{\delta}(f_i), \boldsymbol{w}(f_i), \mu^2(f_i)\right) \\ &= \left\langle \mathrm{In}P\left(\bar{\boldsymbol{X}}'(f_i), \bar{\boldsymbol{S}}(f_i); \boldsymbol{\delta}(f_i), \boldsymbol{w}(f_i), \mu^2(f_i)\right)\right\rangle \\ &= \left\langle \mathrm{In}P\left(\bar{\boldsymbol{X}}'(f_i)\middle|\bar{\boldsymbol{S}}(f_i); \boldsymbol{w}(f_i), \mu^2(f_i)\right) + \mathrm{In}P(\bar{\boldsymbol{S}}(f_i); \boldsymbol{\delta}(f_i))\right\rangle \\ &= \Bigg\langle -M \times KP \times \mathrm{In}\mu^2(f_i) - \mu^{-2}(f_i)\left\|\bar{\boldsymbol{X}}'(f_i) - \boldsymbol{W}(f_i)\boldsymbol{A}(f_i, \boldsymbol{\Omega})\bar{\boldsymbol{S}}(f_i)\right\|_2^2 \\ & \quad - \sum_{l=1}^{L}\left(KP \times \mathrm{In}\delta_l(f_i) + \frac{\left(\sum_{kp=1}^{KP}\left|\bar{S}_l(f_i, kp)\right|^2\right)}{\delta_l(f_i)}\right)\Bigg\rangle \end{aligned} \tag{21}$$

In the M-step, solve derivatives of $F(\bar{\boldsymbol{X}}'(f_i), \bar{\boldsymbol{S}}(f_i); \boldsymbol{\delta}(f_i), \boldsymbol{w}(f_i), \mu^2(f_i))$ for each parameter, that is

$$\begin{aligned} &\frac{\partial F(\bar{\boldsymbol{X}}'(f_i), \bar{\boldsymbol{S}}(f_i); \boldsymbol{\delta}(f_i), \boldsymbol{w}(f_i), \mu^2(f_i))}{\partial \boldsymbol{w}(f_i)} \\ &= -2\mu^{-2}(f_i)\left[\left\langle \boldsymbol{\Lambda}^H(f_i)\boldsymbol{\Lambda}(f_i)\right\rangle \boldsymbol{w}(f_i) - \left\langle \boldsymbol{\Lambda}^H(f_i)(\bar{\boldsymbol{X}}'(f_i) - \boldsymbol{A}(f_i, \boldsymbol{\Omega})\bar{\boldsymbol{S}}(f_i))\right\rangle\right] \end{aligned} \tag{22}$$

$$\begin{aligned} &\frac{\partial F(\bar{\boldsymbol{X}}'(f_i), \bar{\boldsymbol{S}}(f_i); \boldsymbol{\delta}(f_i), \boldsymbol{w}(f_i), \mu^2(f_i))}{\partial \mu^2(f_i)} \\ &= -\frac{M \times KP}{\mu^2(f_i)} + \frac{1}{(\mu^2(f_i))^2}\left\langle \left\| \bar{\boldsymbol{X}}'(f_i) - \boldsymbol{A}'(f_i, \boldsymbol{\Omega})\bar{\boldsymbol{S}}(f_i) \right\|_2^2 \right\rangle \end{aligned} \tag{23}$$

$$\frac{\partial F(\bar{\boldsymbol{X}}'(f_i), \bar{\boldsymbol{S}}(f_i); \boldsymbol{\delta}(f_i), \boldsymbol{w}(f_i), \mu^2(f_i))}{\partial \delta_l(f_i)} = -\frac{KP}{\delta_l(f_i)} + \frac{1}{\delta_l^2(f_i)}\left\langle \sum_{kp=1}^{KP} \left|\bar{S}_l(f_i, kp)\right|^2 \right\rangle \tag{24}$$

Set them to be 0 respectively, the estimation of every parameter of the $p$th iteration is

$$\boldsymbol{w}^{(p)}(f_i) = \left\langle \boldsymbol{\Lambda}^H(f_i)\boldsymbol{\Lambda}(f_i)\right\rangle^{-1}\left\langle \boldsymbol{\Lambda}^H(f_i)(\bar{\boldsymbol{X}}'(f_i) - \boldsymbol{A}(f_i, \boldsymbol{\Omega})\bar{\boldsymbol{S}}(f_i))\right\rangle \tag{25}$$

$$\left(\mu^2(f_i)\right)^{(p)} = \frac{1}{M \times KP}\left\langle \left\| \bar{\mathbf{X}}'(f_i) - (\mathbf{A}'(f_i, \boldsymbol{\Omega}))^{(p)}\bar{\mathbf{S}}(f_i) \right\|_2^2 \right\rangle \tag{26}$$

$$\delta_l^{(p)}(f_i) = \frac{1}{KP}\left\langle \sum_{kp=1}^{KP} \left|\bar{S}_l(f_i, kp)\right|^2 \right\rangle \tag{27}$$

Here $(p)$ denotes number of iterations, after several times, $\boldsymbol{w}(f_i)$, $\mu^2(f_i)$ and $\delta_l(f_i)$ tend to be zero, then they are deemed to be convergent, we can acquire their final estimation: $\hat{\boldsymbol{w}}(f_i)$, $\hat{\mu}^2(f_i)$ and $\hat{\delta}_l(f_i)$. We can use them for array calibration, define $\boldsymbol{X}$ as the vector composed by sum of signal of all frequencies, as the signal of every frequency is independent of one another, the joint probability density of $\boldsymbol{X}$ is

$$\begin{aligned} P(\boldsymbol{X}) &= \prod_{i=1}^{J} P\left(\bar{\boldsymbol{X}}'(f_i); \hat{\boldsymbol{\delta}}(f_i), \hat{\boldsymbol{w}}(f_i), \hat{\mu}^2(f_i)\right) \\ &= |\pi|^{-J \times KP}\prod_{i=1}^{J}\left|\left(\hat{\mu}^2(f_i)\boldsymbol{I}_M + \boldsymbol{A}'(f_i, \boldsymbol{\Omega})\hat{\boldsymbol{\Sigma}}(f_i)(\boldsymbol{A}'(f_i, \boldsymbol{\Omega}))^H\right)\right|^{-KP} \\ &\times \exp\left\{-KP \times \sum_{i=1}^{J} \operatorname{tr}\left(\begin{pmatrix} \hat{\mu}^2(f_i)\boldsymbol{I}_M + \boldsymbol{A}'(f_i, \boldsymbol{\Omega}) \times \\ \hat{\boldsymbol{\Sigma}}(f_i)(\boldsymbol{A}'(f_i, \boldsymbol{\Omega}))^H \end{pmatrix}^{-1} \bar{\boldsymbol{R}}'(f_i)\right)\right\} \end{aligned} \tag{28}$$

Solve logarithm operation on (28), we have

$$\begin{aligned} &\mathrm{In}(P(\mathbf{X})) \\ &= -J \times KP \times \mathrm{In}\pi - KP \times \left( \sum_{i=1}^{J} \mathrm{In}\left| \hat{\mu}^2(f_i)\mathbf{I}_M + \mathbf{A}'(f_i,\boldsymbol{\Omega})\hat{\Sigma}(f_i)(\mathbf{A}'(f_i,\boldsymbol{\Omega}))^{\mathrm{H}} \right| \right) \\ &\quad - KP \times \sum_{i=1}^{J} \mathrm{tr}\left( \begin{pmatrix} \hat{\mu}^2(f_i)\mathbf{I}_M + \mathbf{A}'(f_i,\boldsymbol{\Omega}) \times \\ \hat{\Sigma}(f_i)(\mathbf{A}'(f_i,\boldsymbol{\Omega}))^{\mathrm{H}} \end{pmatrix}^{-1} \bar{\boldsymbol{R}}'(f_i) \right) \end{aligned} \tag{29}$$

Solve the partial differentiation of $\mathrm{In}(P(\boldsymbol{X}))$ with regard to $\boldsymbol{\alpha}$

$$\frac{\partial \mathrm{In}(P(\boldsymbol{X}))}{\partial \boldsymbol{\alpha}} = 0 \tag{30}$$

Combing (29) with (30), we have

$$\hat{\alpha}_k = \arg\max_{\alpha_k} \left| \mathrm{Re}\left\{ \begin{array}{l} \sum_{i=1}^{J} \left[ \left( (\boldsymbol{a}'(f_i,\alpha_k))^{\mathrm{H}} \times \begin{pmatrix} \hat{\mu}^2(f_i)\boldsymbol{I}_M + \boldsymbol{A}'(f_i,\boldsymbol{\Omega}_{-k}) \times \\ \hat{\boldsymbol{\Sigma}}_{-k}(f_i)(\boldsymbol{A}'(f_i,\boldsymbol{\Omega}_{-k}))^{\mathrm{H}} \end{pmatrix}^{-1} \right) \right] \\ \times \left[ \sum_{i=1}^{J} \begin{pmatrix} \boldsymbol{a}'(f_i,\alpha_k)(\boldsymbol{a}'(f_i,\alpha_k))^{\mathrm{H}} \times \\ \left( \begin{pmatrix} \hat{\mu}^2(f_i)\boldsymbol{I}_M + \boldsymbol{A}'(f_i,\boldsymbol{\Omega}_{-k}) \times \\ \hat{\boldsymbol{\Sigma}}_{-k}(f_i)(\boldsymbol{A}'(f_i,\boldsymbol{\Omega}_{-k}))^{\mathrm{H}} \end{pmatrix}^{-1} \bar{\boldsymbol{R}}'(f_i) \right) \end{pmatrix} - \sum_{i=1}^{J} \left( \bar{\boldsymbol{R}}'(f_i) \begin{pmatrix} \begin{pmatrix} \hat{\mu}^2(f_i)\boldsymbol{I}_M + \\ \boldsymbol{A}'(f_i,\boldsymbol{\Omega}_{-k})\hat{\boldsymbol{\Sigma}}_{-k}(f_i) \times \\ (\boldsymbol{A}'(f_i,\boldsymbol{\Omega}_{-k}))^{\mathrm{H}} \end{pmatrix}^{-1} \times \\ \boldsymbol{a}'(f_i,\alpha_k)(\boldsymbol{a}'(f_i,\alpha_k))^{\mathrm{H}} \end{pmatrix} \right) \right] \\ \times \sum_{i=1}^{J} \left[ \begin{pmatrix} \hat{\mu}^2(f_i)\boldsymbol{I}_M + \boldsymbol{A}'(f_i,\boldsymbol{\Omega}_{-k}) \times \\ \hat{\boldsymbol{\Sigma}}_{-k}(f_i)(\boldsymbol{A}'(f_i,\boldsymbol{\Omega}_{-k}))^{\mathrm{H}} \end{pmatrix}^{-1} \times \frac{\partial \boldsymbol{a}'(f_i,\alpha_k)}{\partial \alpha_k} \right] \end{array} \right\} \right|^{-1} \tag{31}$$

Thus, the DOA can be estimated.

We will obtain $\rho_2(f_i)\mathrm{e}^{\mathrm{j}\varphi_2(f_i)}, \cdots, \rho_M(f_i)\mathrm{e}^{\mathrm{j}\varphi_M(f_i)}$ according to $\hat{\boldsymbol{w}}(f_i)$, thus $\boldsymbol{W}(f_i)$ can be calculated by (11) and (12), then $\boldsymbol{a}'(f_i,\alpha_k)$ and $\boldsymbol{A}'(f_i,\boldsymbol{\Omega}_{-k})$ can be acquired, we will get the accurate estimation based on (31) and the parameters above.

The method is used for wideband signal, and has employed spatial domain sparse optimization for gain and phase errors, so we can call it WSGP for short.

## 4 Simulations

Here, some simulations are presented for the method, consider some wideband chirp signals impinge on a uniform linear array with 8 omnidirectional sensors from $(16°, 28°, 35°)$, the center frequency of the signals is 2 GHz, width of the band is 20% of the center frequency, the band is divided into 10 frequencies, and spacing $d$ between adjacent sensors is equal to half of the wavelength of the center frequency. Now we will simplify the generation process of the error, suppose the gain and phase uncertainties are respectively selected between $(0 \sim 2)$ and $(-45° \sim 45°)$ randomly.

**Table 1.** Gain and phase errors estimation

| | Actual error at $f_1$ | Estimated error at $f_1$ | Actual error at $f_2$ | Estimated error at $f_2$ |
|---|---|---|---|---|
| $gp_2$ | −0.185+j0.159 | −0.246+j0.106 | 0.585+j0.079 | 0.527+j0.031 |
| $gp_3$ | 0.189−j0.015 | 0.122−j0.073 | 0.635+j0.951 | 0.584+j1.104 |
| $gp_4$ | 0.209+j0.197 | 0.270+j0.261 | −0.451+j0.606 | −0.513+j0.661 |
| $gp_5$ | 0.665−j0.681 | 0.719−j0.617 | 0.855+j0.376 | 0.798+j0.422 |
| $gp_6$ | 0.823+j0.267 | 0.761+j0.195 | 0.377+j0.167 | 0.329+j0.224 |
| $gp_7$ | 0.506+j0.343 | 0.562+j0.402 | −0.559−j0.403 | −0.615−j0.358 |
| $gp_8$ | 0.637+j0.203 | 0.795+j0.151 | 0.351+0.195 | 0.406+j0.249 |
| | Actual error at $f_3$ | Estimated error at $f_3$ | Actual error at $f_4$ | Estimated error at $f_4$ |
| $gp_2$ | 0.529+j0.357 | 0.486+j0.322 | −0.805+j0.227 | −0.772+j0.205 |
| $gp_3$ | 0.833+j0.228 | 0.797+j0.262 | 0.517+j0.201 | 0.488+j0.183 |
| $gp_4$ | −0.918+j0.219 | −0.884+j0.265 | 0.252+j0.192 | 0.226+j0.221 |
| $gp_5$ | −0.663−j0.135 | −0.616−j0.102 | −0.478−j0.220 | −0.501−j0.256 |
| $gp_6$ | 0.388+j0.276 | 0.425+j0.238 | 0.804+j0.184 | 0.768+j0.204 |
| $gp_7$ | −0.489+j0.535 | −0.443+j0.496 | −0.566+j0.380 | −0.542+j0.346 |
| $gp_8$ | 0.742+j0.048 | 0.708+j0.005 | 0.309+j0.148 | 0.279+j0.117 |
| | Actual error at $f_5$ | Estimated error at $f_5$ | Actual error at $f_6$ | Estimated error at $f_6$ |
| $gp_2$ | 0.391+j0.742 | 0.372+j0.763 | 0.703+j0.443 | 0.726+j0.429 |
| $gp_3$ | −0.836−j0.568 | −0.821−j0.589 | 0.492+j0.562 | 0.478+j0.539 |
| $gp_4$ | 0.185+j0.477 | 0.206+j0.455 | 0.678+j0.360 | 0.658+j0.345 |
| $gp_5$ | −0.516−j0.344 | −0.541−j0.357 | 0.291+j0.124 | 0.267+j0.143 |
| $gp_6$ | −0.348−j0.342 | −0.352−j0.291 | 0.599+j0.549 | 0.623+j0.537 |
| $gp_7$ | 0.571+j0.464 | 0.543+j0.447 | 0.410+j0.166 | 0.392+j0.183 |
| $gp_8$ | 0.293+j0.255 | 0.274+j0.273 | 0.231+j0.197 | 0.219+j0.215 |
| | Actual error at $f_7$ | Estimated error at $f_7$ | Actual error at $f_8$ | Estimated error at $f_8$ |
| $gp_2$ | 0.331+j0.290 | 0.348+j0.317 | 0.663+j0.991 | 0.625+j0.959 |
| $gp_3$ | 0.669+j0.212 | 0.643+j0.186 | 0.888+j0.612 | 0.846+j0.570 |
| $gp_4$ | −0.578+j0.619 | −0.605+j0.645 | 0.292+j0.157 | 0.321+j0.206 |
| $gp_5$ | 0.243+j0.517 | 0.272+j0.546 | −0.701+j0.447 | −0.660+j0.409 |
| $gp_6$ | 0.490+j0.318 | 0.518+j0.353 | 0.479+0.686 | 0.426+j0.649 |
| $gp_7$ | 0.547+j0.202 | 0.512+j0.233 | −0.147+j0.413 | −0.186+j0.372 |
| $gp_8$ | 0.479+j0.114 | 0.511+j0.148 | 0.958+j0.391 | 0.906+j0.369 |
| | Actual error at $f_9$ | Estimated error at $f_9$ | Actual error at $f_{10}$ | Estimated error at $f_{10}$ |
| $gp_2$ | −0.421+j0.879 | −0.372+j0.937 | 0.471-j0.763 | 0.525-j0.707 |
| $gp_3$ | 0.597+j0.430 | 0.548+j0.382 | 0.751+j0.116 | 0.697+j0.053 |
| $gp_4$ | 0.554+j0.169 | 0.605+j0.123 | −0.585-j0.224 | −0.642-j0.166 |
| $gp_5$ | 0.667+j0.297 | 0.624+j0.232 | −0.195-j0.524 | −0.266-j0.463 |
| $gp_6$ | −0.234+j0.212 | −0.285+j0.266 | 0.461+j0.288 | 0.409+j0.343 |
| $gp_7$ | 0.716+0.330 | 0.658+0.287 | 0.352+j0.662 | 0.427+j0.703 |
| $gp_8$ | −0.502-j0.249 | −0.456-j0.305 | 0.727+j0.165 | 0.668+j0.225 |

### 4.1 Gain and Phase Errors Estimation

Suppose SNR is 10dB, the number of samples at every frequency is 30, WSGP is employed for estimating gain and phase errors, 200 Monte-Carlo simulations are repeated, their average is deemed as the final results, the estimation errors of every frequency are shown in Table 1.

Table 1 shows the method can effectively estimate the gain and phase errors existing in the array, especially when the frequency is near to the center bin, we can use these results to calibrate the array and obtain the DOA.

### 4.2 DOA Estimation

First, traditional two-sided correlation transformation (TCT) [17] and WSGP methods are employed for estimating DOA of wideband signals along with the gain and phase errors above, here, TCT is performed without correction, the estimation error of DOA is defined as $\sum_{k=1}^{K} |\alpha_k - \hat{\alpha}_k|$. 200 Monte-Carlo simulations are repeated, their average values are deemed as the final results. Suppose samples of every frequency is 30, other conditions are the same with 4.1, estimation error versus SNR are shown in Fig. 2; then suppose SNR is 10dB, that versus number of samples are shown in Fig. 3.

Figures 2 and 3 show that WSGP can effectively estimate the DOA of wideband signals along with the gain and phase errors, the estimation error approximately converges to 0.7° at last, but that of the traditional TCT method without correction converges to 1.6° under the same condition.

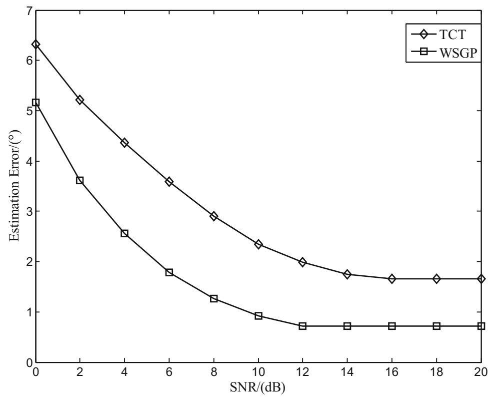


**Fig. 2.** Calibration Accuracy versus SNR

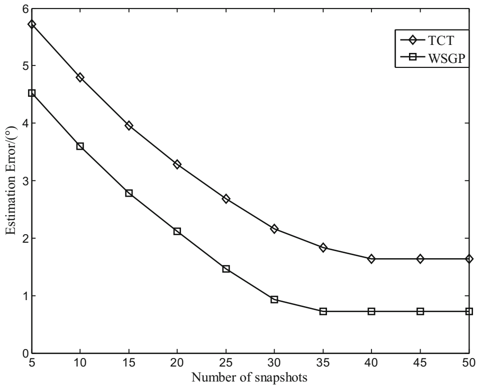


**Fig. 3.** Calibration Accuracy versus number of snapshots

# 5 Conclusion

The paper proposed a novel array calibration method in super-resolution direction finding for wideband signals based on spatial domain sparse optimization to the gain and phase errors existing in the array, it can calibrate the array and estimate the DOA relatively accurately.

**Acknowledgments.** I would like to thank Heilongjiang province ordinary college electronic engineering laboratory and post doctoral mobile stations of Heilongjiang University.

# References

1. Muhammad, M.R., Iftekharuddin, K.M., Ernest, M.: Autonomous wireless radar sensor mote for target material classification. J. Digit. Sig. Process. **23**, 722–735 (2013)
2. Soh, P.J., Vanden, B.B., Xu, H.T.: A smart wearable textile array system for biomedical telemetry applications. J. IEEE Trans. Microw. Theory Tech. **61**, 2253–2261 (2013)
3. William, R.O., Aniruddha, G., Schmidt, D.C.: Efficient and deterministic application deployment in component-based enterprise distributed real-time and embedded systems. J. Inform. Softw. Technol. **55**, 475–488 (2013)
4. Mehmet, B., Guldogan, O.A.: A new technique for direction of arrival estimation for ionospheric multipath channels. J. Adv. Space Res. **44**, 653–662 (2009)
5. Muhammad, S., Ghulam, A.H.: Partial discharge diagnostic system for smart distribution networks using directionally calibrated induction sensors. J. Electr. Power Syst. Res. **119**, 447–461 (2015)
6. Li, J., Zhao, Y.J., Li, D.H.: Accurate single-observer passive coherent location estimation based on TDOA and DOA. J. Chin. J. Aeronaut. **27**, 913–923 (2014)
7. Giuseppe, F., Andrew, H.: A multipath-driven approach to HF geolocation. J. Sig. Process. **93**, 3487–3503 (2013)
8. Luis, S., Luis, M., Jose, A.G.: SmartSantander: IoT experimentation over a smart city testbed. J. Comput. Netw. **61**, 217–238 (2014)

9. Verdouw, C.N., Beulens, A.J.M., van der Vorst, J.G.A.J.: Virtualisation of floricultural supply chains: a review from an Internet of things perspective. J. Comput. Electr. Agric. **99**, 160–175 (2013)
10. Srinath, H., Reddy, V.U.: Analysis of MUSIC algorithm with sensor gain and phase perturbations. J. Sig. Process. **23**, 245–256 (1991)
11. Schmidt, R.O.: Multiple emitter location and signal parameter estimation. J IEEE Trans. Antennas Propag. **34**, 276–280 (1986)
12. Wang, T.D., Liao, H.S., Li, L.P.: Fast DOA estimation with ULA in the presence of sensor gain and phase errors. In: 2009 International Conference on Communications, Circuits and Systems, pp. 395–397. Milpitas (2009)
13. Jiang, J.J., Duan, F.J., Chen, J.: Two new estimation algorithms for sensor gain and phase errors based on different data models. IEEE Sens. J. **13**, 1921–1930 (2012)
14. Xu, L., Zeng, C., Liao, G.S.: DOA estimation for strong and weak signals in the presence of array gain and phase mismatch. In: 2010 International Conference on Multimedia Technology, pp. 1–4. Ningbo (2010)
15. Cao, S.H., Ye, Z.F., Hu, N., Xu, X.: DOA estimation based on fourth-order cumulants in the presence of sensor gain-phase errors. J. Sig. Process. **93**, 2581–2585 (2013)
16. Dempster, A.P., Laird, N.M., Rubin, D.B.: Maximum likelihood from incomplete data via the EM algorithm. J. R. Stat. Soc. **39**, 1–38 (1977)
17. Valaee, S., Kabal, P.: Wideband array processing using a two-sided correlation transformation. J. IEEE Trans. Sig. Process. **43**, 160–172 (1995)